water

MDPI

Article

Integrated GIS, Remote Sensing, and Electrical Resistivity Tomography Methods for the Delineation of Groundwater Potential Zones in Sangaw Sub-Basin, Sulaymaniyah, KRG-Iraq

Azad Sangawi , Diary Ali Mohammed Al-Manmi * and Bakhtiar Qader Aziz

Department of Geology, University of Sulaimani, Sulaymaniyah 46001, Iraq
* Correspondence: diary.amin@univsul.edu.iq; Tel.: +964-770-146-1311

Abstract: In the Sangaw region, groundwater is the primary supply of water for drinking, residential purposes, livestock, and summer farming activities. Therefore, the main objective of this research is to delineate groundwater potential zones (GWPZs) in the Sangaw sub-basin, Sulaymaniyah, KRG-Iraq, by integrating geographic information system (GIS), remote sensing (RS), analytical hierarchy process (AHP), and electrical resistivity tomography (ERT) techniques. Seven different thematic layers, including geology, rainfall, slope, lineament density, land use/land cover, drainage density, and topographic position index, were chosen as the prediction factors. The analytical method of an analytical hierarchy process pair-wise matrix was used to evaluate the normalized weight of these thematic layers. All the layers and their corresponding classes were assigned ranks and weights based on their impact on groundwater potential. Using ArcGIS, these thematic maps were combined to precisely determine the groundwater potential map within the research area. Five different potential zones were generated for the resulting map, namely, very low (55.4 km^2), low (90.4 km^2), moderate (68.1 km^2), high (100 km^2), and very high (62.4 km^2). The findings revealed that almost 43.2% of the study region is characterized by high to very high groundwater potential zones. In contrast, the very low to low groundwater potential covers around 38.7%, and the moderate groundwater potential occupies 18.1% of the study region. The final map was then validated using results from the two-dimensional inverse sections of eight electrical resistivity tomography profiles. The validation data confirmed that groundwater potential classes strongly overlap with the subsurface water-bearing or non-bearing lithology, and groundwater productivity zones in the given area. The novelty of this research lies in the application of electrical resistivity tomography validation to the groundwater potential mapping approach, which illustrates the robustness of the overall methodology for data-scarce areas. Furthermore, this is one of the very few groundwater potential studies in Iraq and the first in the Sangaw sub-basin, which can assist decision-makers with groundwater prospecting and management, and enable further exploration in the region.

Keywords: GIS and remote sensing; electrical resistivity tomography; groundwater potential; analytical hierarchy process; Sangaw

Citation: Sangawi, A.; Al-Manmi, D.A.M.; Aziz, B.Q. Integrated GIS, Remote Sensing, and Electrical Resistivity Tomography Methods for the Delineation of Groundwater Potential Zones in Sangaw Sub-Basin, Sulaymaniyah, KRG-Iraq. *Water* **2023**, *15*, 1055. https://doi.org/10.3390/w15061055

Academic Editor: Aldo Fiori

Received: 28 January 2023
Revised: 18 February 2023
Accepted: 21 February 2023
Published: 10 March 2023

1. Introduction

Groundwater is considered among the most valuable essential of natural resources as it forms a reliable water supply source in all climatic areas of all over the world [1–3]. The phrase "groundwater potential" can be described from the perspective of groundwater exploration as the possibility for groundwater that exists in a region [4]. In arid to semi-arid environments, such as Iraq, groundwater resources are the most in demand to supply water for population, industry, and agricultural uses [5,6]. By 2005, Iraq began to suffer a sharp decline in its capacity to satisfy its water demand. By 2035, the country will hit a wall; it will not have enough freshwater of sufficient quantity and quality to meet its development needs [7–9]. In this area, water shortage combined with groundwater exploitation is a major concern. Therefore, the exploration of groundwater resources and the concept of its sustainability become indispensable. Although the difficulty of managing groundwater is significantly increased, these areas face a lack of adequate data [10]. Unfortunately, surface water resources are insufficient to satisfy current water demands [11]. Nevertheless, in many areas surface water cannot be considered a reliable source as it is highly susceptible to seasonal variations and pollution from anthropogenic sources [12,13], especially in the Sangaw sub-basin, as a result of the lack of permanent streams, insufficient precipitation, hot climatic conditions, and presence of sulfur and halite composition. Therefore, Sangaw town and the more than 30 surrounding villages rely mostly on groundwater for drinking, residential usage, livestock, and agricultural activities in the summer.

A literature review shows that researchers around the world have employed a wide variety of techniques to delineate groundwater potential zones. The most commonly used methods in this field are analytic hierarchy process (AHP) [14], frequency ratio [15], weights of evidence [16], and logistic regression [17]. Moreover, a wide range of machine learning-based methods is now widely employed for defining GWPZs. These are Naïve Bayes [18], Artificial Neural Network and Support Vector Machine [19], Boosted Regression Trees [20], Classification and Regression Tree [21], Linear Discriminant Analysis [22], and Random Forest [21].

In the last few decades, numerous studies have revealed that multi-criteria decision analysis (MCDA) methodologies are useful for creating a framework to manage groundwater resources [4,23–25]. The analytical hierarchy process offers a flexible, minimal-cost, and easily comprehended technique for analyzing complex issues [26]. Curiously, the AHP approach allows experts to remark on the relative significance of thematic maps for determining groundwater potential zones [27–30]. Hajkowicz et al. [31] investigated the application of the MCDA techniques that can be used in managing water resources and demonstrated that the AHP is widely used and developing. According to Chenini et al. [32], mapping the groundwater recharge zone can be done effectively using the MCDA technique with the aid of GIS. Furthermore, GIS and RS have been recognized as very effective methods for monitoring, managing, and evaluating groundwater resources [33–37]. The successful strategy that can simplify complex decisions into a series of pair-wise comparisons is the integration of GIS with AHP, suggested by Thomas Saaty in 1980 [38,39]. The AHP and GIS approaches have been extensively employed in groundwater potential evaluation, as can be seen in the abovementioned literature. These methods have some shortcomings in spite of being used in different parts of the globe. However, the major cause of uncertainty in AHP is that it relies heavily on expert knowledge [40].

A single technique for identifying groundwater potential zones is currently insufficient to support the research. In addition, geophysical methods, including electrical resistivity tomography, can be an accurate alternative for evaluating and validating the groundwater potential zones. Therefore, some researchers have successfully combined GIS with geophysical techniques for groundwater potential mapping investigations [41–48]. The most common and economical geophysical method for groundwater prospecting is geoelectrical resistivity [42]. The technique has developed remarkable progress in its application over the past years. Kowalsky et al. [49] stated that the main ideas behind this method are based on the electrical resistivity of the geological rock units and their water content and porosity.

Research on groundwater potential mapping in the Sangaw sub-basin has not been conducted up to this point. Therefore, an integration of GIS, remote sensing, hydrogeological data, and geophysical studies is required to understand the availability of groundwater and subsurface lithology in the region. The main objective of this study is to identify the potential zones of groundwater in the Sangaw sub-basin using an integration of geographic information systems, remote sensing, and analytical hierarchy process, and verify the result by two-dimensional electrical resistivity tomography. In a data-scarce area, such as Iraq, the application of electrical resistivity tomography as a validation tool to assess the groundwater potential map result is considered one of the novel aspects of this research.

Moreover, the research is expected to provide a comprehensive scientific basis for further groundwater investigation and development in the study area.

2. Materials and Methods

2.1. Area of Study

Sangaw sub-basin has been chosen to delineate the GWPZs, which is about 40 km to the southwest of Sulaymaniyah Governorate in the Iraqi Kurdistan Region. Geographically, it is bounded by the north latitudes (35°7′41.878′′–35°23′0.956′′) and east longitudes (45°13′44.581′′–45°20′5.194′′), as displayed in Figure 1. Moreover, the research area occupies approximately 378.3 km^2, and the altitude of the region varies from 550 to 1856 m above sea level. According to [50,51], the research region has a continental arid to semi-arid climate and is locally called the Garmyan (hot) region, with long warm summers and cold winters. Rainfall in the region typically occurs from October to May, with a dry period in the summer months of June, July, and August. Rainfall data has been collected from the Sangaw Agricultural Directorate, which is the only available rainfall station in the study area, and the average annual rainfall of the site between 2001–2002 and 2021–2022 is 483 mm. In a subtropical region, such as all territories of Iraq, including the research area, rainfall data can be collected from the Tropical Rainfall Measuring Mission (TRMM), which was a shared space mission between the Japan Aerospace Exploration Agency and NASA [52].

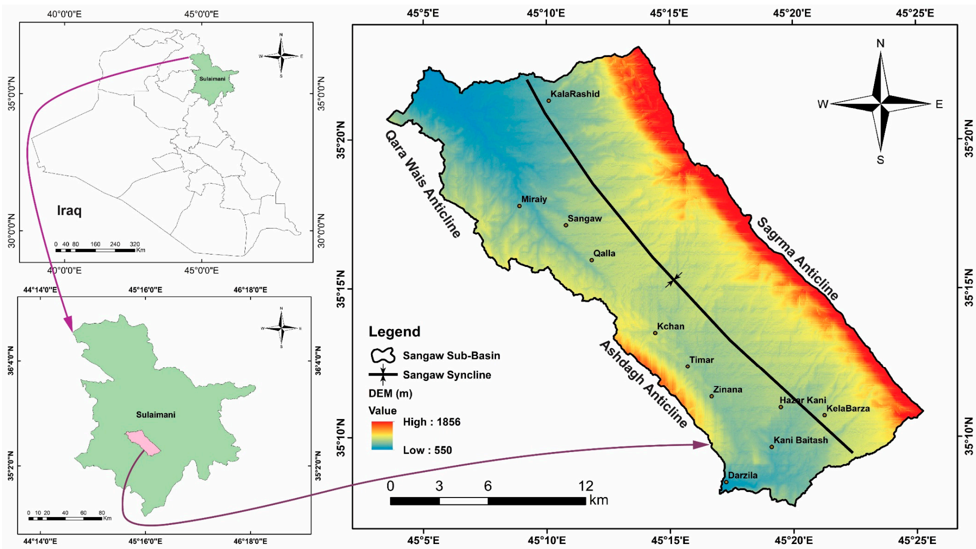

Figure 1. Location map of the study area.

2.2. Geological and Hydrogeological Settings

Geological formations of the study area are distinguished by the exposure of ten various rock units dating from the Late Eocene period to the Pleistocene period [53–56]. Within the studied area, the dominant formations are Fatha, Injana, and recent sediments, which are composed of different rock units and cover most parts of the area, as demonstrated in Table 1. The occurrence of Oligocene rocks is rarely reported around Sargrma mountain, while they become thicker toward the Ashdagh anticlines. In addition, the rock units of the Oligocene are spatially visible and developed with varying thicknesses [57]. Only the presence of Shurau, Bajawan, Baba, Euphrates, and Jeribe formations were confirmed around Timar village in the NE limb of Ashdagh mountain, as shown in Figure 2.

Table 1. Lithological characteristics of the existing formations in the study area.

Epoch	Formations	Lithological Properties	Coverage Area (%)
Pleistocene	Recent deposit	Conglomerate, Sandstone, claystone, and limestone fragment	34.1
L. Miocene	Injana	Alternation of thick-bedded red claystone with grey sandstone	25.2
M. Miocene	Fatha	Alternation of gypsum, marl, sandstone, and claystone	24.9
Oligocene-E. Miocene	Shurau, Baba, Bajawan, Euphrates, Dhiban, Jeribe	Mostly composed of massive limestone, dolomitized limestone, thin marl	4.4
L. Eocene	Pila Spi Formation	Chalky and dolomitic Limestone	11.4

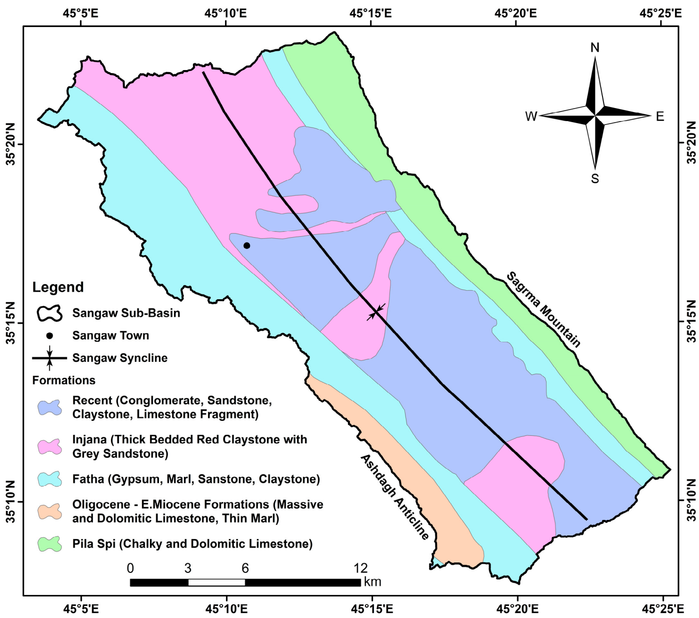

Figure 2. Geological map of the study area.

The study area is situated within the Chamchamal–Sangaw basin from a hydrological perspective. The main aquifer system is the highly fissured, well-karstified Pila Spi aquifer in the center of the Ashdagh anticline. There is also a local aquifer system in Oligocene rocks with visible features, channels, and caves [58,59]. Moreover, the recent deposit is another important unit regarding hydrogeological characteristics and water availability, which provides water supply for most of the residents in the region. Fatha and Injana Formations are less productive water-bearing layers that are tapped by wells and are characterized by poor water quality due to evaporate leaching [60].

2.3. Used Data Set and Thematic Layers Preparation

Combining remote sensing, GIS, and AHP approaches is a technique for transforming and integrating weighted rankings with geographic data to produce information for the decision-maker [61,62]. Table 2 displays the data sources utilized to define the GWPZs.

Table 2. Details of source data in this study.

Thematic Layers	Resolution Scale	Data and Source
Geology (Ge)	1:250,000	Provided by Iraqi geological survey maps, [63,64]
Rainfall (Rf)	0.25° 0.25°	TRMM rainfall data, Type-3B43-V7, [65]
Lineament density (Ld)	30 m	Generated from STRM DEM and Landsat 8
Slope (Sp)	30 m	Generated from STRM DEM
Drainage density (Dd)	30 m	Generated from STRM DEM
LULC (Lu)	30 m	Generated from Landsat 8 and provided by Iraqi Geological Survey [66]
Topographic Position Index (TPI)	30 m	Generated from STRM DEM

The TRMM rainfall data (Type-3B43-V7), which integrates precipitation with a pixel size of 0.25°x 0.25°, has been used to create the rainfall map because of the scarcity of available gauging stations in the Sangaw region. Precipitation data (TRMM) is available from January 1998 to December 2019, and the applicability of TRMM data in the study area was determined by comparing it to the recorded precipitation dataset of the Sangaw Agricultural Weather Station. From September 2001 to December 2019, 166 recorded precipitation readings were used. Figure 3 shows a reasonable linear correlation between the observed precipitation and the monthly TRMM dataset, where the determination coefficient (R^2), slope, and intercept were 0.669, 0.7942, and 23.5985, respectively. Finally, an inverse distance weighted (IDW) interpolation tool in ArcGIS 10.8 was used to define the geographical distribution map of precipitation. Figure 4 illustrates the overall methodological flowchart of the study.

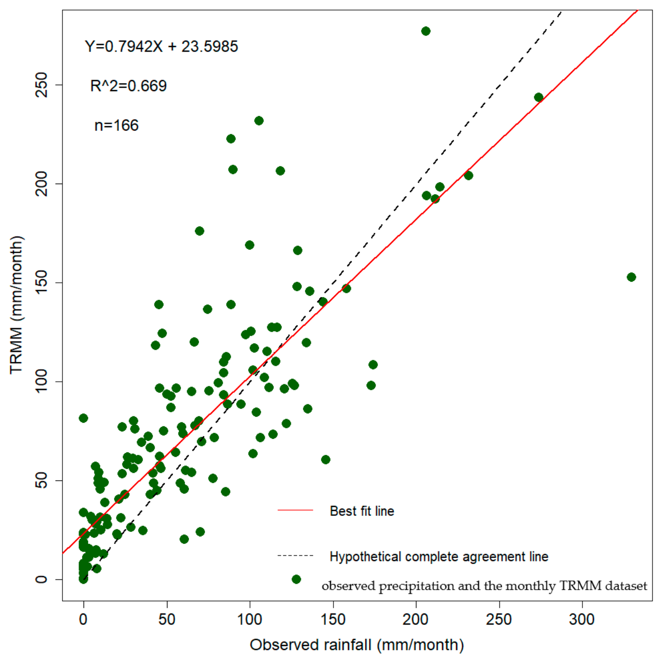

Figure 3. Recorded rainfall data comparison from Sangaw Agricultural Weather Station versus TRMM data for the same pixel from September 2001 to December 2019.

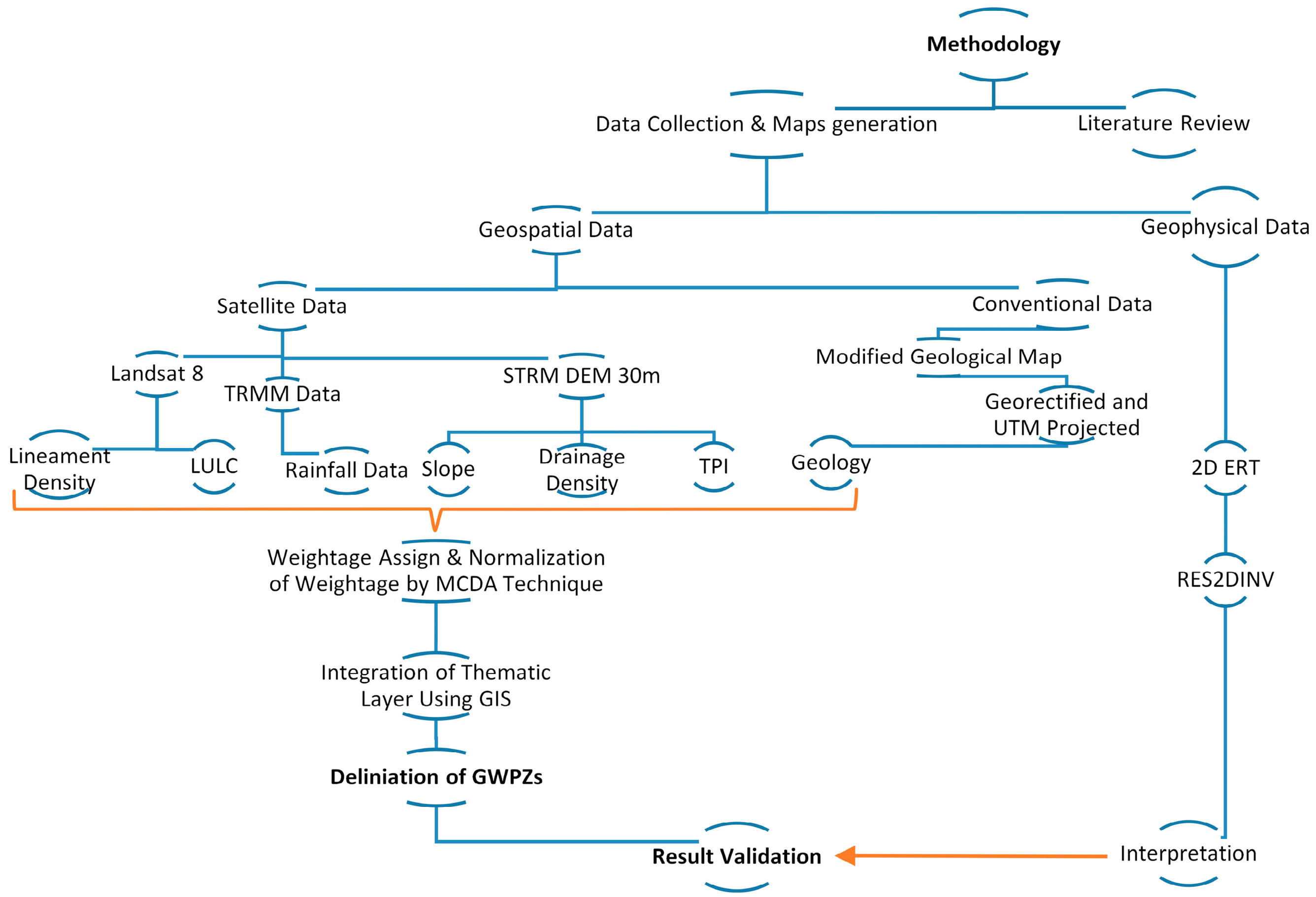

Figure 4. Flowchart displaying methodology adapted for delineating the GWPZs.

2.4. Assignment and Normalization of Weights

Multi-criteria decision analysis (MCDA) using the Analytical Hierarchical Process is the most popular and widely used GIS-based technique for defining groundwater potential zones. The AHP is useful for determining criteria weight through comparative analysis [26,67]. As a principle of assessment by pairwise comparison matrix (PCM), the AHP uses the knowledge of experts and the literature reviews of many researchers [62,68]. Weights were allocated based on groundwater recharge potential. A thematic layer with a high weight demonstrates a layer with great influence, and a thematic layer with a low weight demonstrates a minor influence on groundwater potential. Table 3 shows the results of a PCM that was used to determine the impact and significance of each theme. According to [69], the values for the thematic layers range from 1 (equal significance) to 9 (extreme significance).

The next step is to normalize and check the consistency ratio of the data. Table 4 illustrates the normalized PCM obtained by dividing each cell by the sum of its column and the normalized weights obtained by averaging all of the rows. The consistency of these weights is then evaluated using the consistency index (CI) and consistency ratio (CR) calculations. The CR is calculated using Equation (1):

$$\mathrm{CR} = \frac{\mathrm{CI}}{\mathrm{RI}} \tag{1}$$

Table 3. Pairwise comparison matrix (PCM) for the seven themes using the AHP technique in Sangaw sub-basin.

Thematic Layers	Thematic Layers						
	Ge	**Rf**	**Ld**	**Sp**	**Dd**	**Lu**	**TPI**
Geology (Ge)	1.00	2.00	3.00	3.00	5.00	5.00	9.00
Rainfall (Rf)	0.50	1.00	2.00	2.00	3.00	3.00	7.00
Lineament density (Ld)	0.33	0.50	1.00	1.00	2.00	2.00	5.00
Slope (Sp)	0.33	0.50	1.00	1.00	2.00	2.00	5.00
Drainage density (Dd)	0.20	0.33	0.50	0.50	1.00	1.00	3.00
LULC (Lu)	0.20	0.33	0.50	0.50	1.00	1.00	3.00
Topographic Position Index (TPI)	0.11	0.14	0.20	0.20	0.33	0.33	1.00
Column total	2.68	4.81	8.20	8.20	14.33	14.33	33.00

Table 4. Normalized pairwise comparison matrix (PCM) for the AHP process in the Sangaw sub-basin.

Thematic Layers	Thematic Layers							Normalized Weights (W)	Percentage Influenced
	Ge	**Rf**	**Ld**	**Sp**	**Dd**	**Lu**	**TPI**		
Geology (Ge)	0.373	0.416	0.366	0.366	0.349	0.349	0.273	0.356	35.6
Rainfall (Rf)	0.187	0.208	0.244	0.244	0.209	0.209	0.212	0.216	21.6
Lineament density (Ld)	0.124	0.104	0.122	0.122	0.140	0.140	0.152	0.129	12.9
Slope (Sp)	0.124	0.104	0.122	0.122	0.140	0.140	0.152	0.129	12.9
Drainage density (Dd)	0.075	0.069	0.061	0.061	0.070	0.070	0.091	0.071	7.1
LULC (Lu)	0.075	0.069	0.061	0.061	0.070	0.070	0.091	0.071	7.1
Topographic Position Index (TPI)	0.041	0.030	0.024	0.024	0.023	0.023	0.030	0.028	2.8
Column total	1.000	1.000	1.000	1.000	1.000	1.000	1.000	1.000	100.0

CR is the consistency ratio, CI is the consistency index, and RI stands for the random index, which was derived from a table created by [69]. It depends on the number of thematic layers, and, in this research, it is equal to 1.32. A consistency ratio of 0.10 or less is satisfactory to continue the analysis. If the CR is higher than 0.10, the judgment needs to be reviewed to identify the root reasons for the inconsistency and make the required corrections. If the CR value is zero, it implies the level of consistency in the pair-wise comparison is perfect [69]. CI is determined by using Equation (2):

$$\mathrm{CI} = \lambda_{\max} - \frac{n}{n} - 1 \tag{2}$$

where λmax is a principal eigenvalue, n is the number of thematic layers, and CI is the consistency index. In this study, the CR is calculated to be 0.006 (λmax = 7.05, n = 7, RI = 1.32, CI = 0.008), which shows a perfect consistency in the pairwise matrix comparison.

2.5. Normalized Weights for Thematic Maps

The characteristics features of each theme were allocated were given a weight value of 1–9 (1 = very low, 3 = low, 5 = moderate, 7 = high, and 9 = very high) based on their impact on groundwater occurrence [38,43,70,71]. All the thematic layers were categorized into features/sub-classes and ranked according to their influence on groundwater potentiality. As demonstrated in Table 5, the normalized ranks of each subclass are calculated by dividing each subclass's rank value by the sum of all ranks.

Table 5. Weights of features/classes of thematic maps for potential groundwater zoning.

Thematic Layers	Features/Classes	Assigned Rank	Groundwater Storage Potentiality	Feature Normalized Weight (Wf)
Geology	Injana Formation	3	Low	0.08
	Fatha Formation	5	Moderate	0.13
	Recent deposit	7	High	0.18
	Pila Spi and Oligocene Formations	9	Very High	0.24
Rainfall	535–552	1	Very Low	0.04
	552–563	3	Low	0.12
	563–574	5	Moderate	0.20
	574–585	7	High	0.28
	585–602	9	Very High	0.36
Lineament density (km/km^2)	0–0.4	1	Very Low	0.04
	0.4–0.92	3	Low	0.12
	0.92–1.33	5	Moderate	0.20
	1.33–1.82	7	High	0.28
	1.82–2.9	9	Very High	0.36
Slope (Degree)	0–5	9	Very High	0.36
	5–10	7	High	0.28
	10–17	5	Moderate	0.20
	17–27	3	Low	0.12
	27–56	1	Very Low	0.04
Drainage density (km/km^2)	0–0.75	9	Very High	0.36
	0.75–1.34	7	High	0.28
	1.34–1.83	5	Moderate	0.20
	1.83–2.33	3	Low	0.12
	2.33–3.45	1	Very Low	0.04
LULC	Vegetated Land and Carbonate Rocks	7	High	0.16
	Burn Land, Cultivated Land, Gypsum, Harvested Land, Mix Barren Land, and other Clastic Rocks	5	Moderate	0.11
	Urban and Built-up Land	1	Very Low	0.02
TPI	(−)102.6–(−)41	9	Very High	0.36
	(−)41–(−)20	7	High	0.28
	(−)20–40	5	Moderate	0.20
	40–115	3	Low	0.12
	115–185.41	1	Very Low	0.04

2.6. Groundwater Potential Zones Identification

Groundwater potential zones (GWPZs) are dimensionless quantities, which support prediction of the potential groundwater zones in a region [25,62,72]. All the thematic maps were combined to generate the possible GWPZs using Equation (3):

$$\mathrm{GPZI} = \mathrm{Ge_w Ge_{wf}} + \mathrm{Rf_w Rf_{wf}} + \mathrm{Ld_w Ld_{wf}} + \mathrm{Sp_w Sp_{wf}} + \mathrm{Dd_w Dd_{wf}} + \mathrm{Lu_w Lu_{wf}} + (\mathrm{TPI_w TPI_{wf}}) \tag{3}$$

where GPZI is groundwater potential index, Ge represents Geology, Rf represents rainfall, Ld represents lineament density, Sp stands represents slope, Dd represents drainage density, Lu represents land use/land cover, TPI represents topographic position index, w denotes theme normalized weight, and wf denotes feature/class normalized weight.

2.7. Validation of Groundwater Potential Map

Electrical resistivity tomography (ERT), as a simplistic and more accurate validation approach, was accepted for assessing the effectiveness of the methodology, as illustrated in Figure 4 [73]. Additionally, ERT is the most popular and accurate geophysical technique for groundwater investigation because of the wide variability in rock resistivity and the changes caused by rock saturation [71]. In addition to validation, ERT is a crucial geophysical tool for groundwater investigation to delineate water-bearing zones, especially in water-scarce areas, such as Sangaw Town. A combined inversion of the Wenner-Schlumberger (WS) configuration has been used to collect ERT data from eight profiles in Sangaw sub-basin to obtain high-resolution resistivity data of subsurface layers, and the features of the hydrogeological condition. All the profiles follow the general strike of the outcrops, which runs roughly from NW to SE. At the NW end, the first electrodes were installed, and at the SE end, electrodes 72. The electrode spacing for each survey was 10 m, the length of each profile was equal to 710 m, and the total number of datum points recorded for every single profile was 677. The software package "RES2DINV" version 4.8.10 is used for 2D inversion analysis and interpretation [43,74–76].

To generate accurate subsurface resistivity models of the region, the observed apparent resistivity field dataset was first processed to remove noisy and poor datum points at various depths. Furthermore, depending on the quality and smoothness of resistivity data, damping factors, convergence limits, and numbers of iterations must be allocated to each dataset [77,78]. Lastly, RES2DINV was used to invert field data up to five iterations, and the absolute error values (ABS) did not exceed 3%.

In light of the limitations of this study, the analytical hierarchy process lacks realism due to the common reliance of assessments on surficial factors, such as topography, exposed lithology, and land use/land cover for mapping, which do not consider the nature of the aquifer. Therefore, some points must be taken into consideration, such as aquifer type, including its classification (unconfined, confined, or semi-confined), hydraulic properties, saturated thickness, groundwater levels, and groundwater quality.

3. Results

3.1. Thematic Layers for GWPZ Mapping in the Study Area

3.1.1. Geology

The rock formations of an area have a significant impact on the distribution pattern of groundwater [62,79]. In the Sangaw region, the main lithological units were delimited based on fieldwork, previous studies, and the existing map of geology, Table 1. Geology is the most significant factor with the weight (W) of 0.356 used to determine GWPZs of the Sangaw sub-basin. The study region (area) was classified into four formation groups depending on their lithological properties, as displayed in Table 5. They are: Late Eocene (Pila Spi) and Early Miocene–Oligocene (Shurau, Bajawan, Baba Euphrates, Dhiban, and Jeribe) formations were ranked with the value of "9" representing a very high potential for groundwater storage. In contrast, the Pleistocene (Recent deposit) was ranked with "7" (high potential), M. Miocene (Fatha) Formation was ranked with "5" (moderate potential), and L. Miocene (Injana) Formation was ranked with "3" (low potential), as shown in Figure 5a. These ranking classes occupy the study area of 15.82%, 34%, 24.95%, and 25.23%, respectively.

3.1.2. Rainfall

Rainfall is considered among the most substantial hydrologic components that crucially impact groundwater recharge [70,80,81]. In the Sangaw sub-basin, natural infiltration of precipitation is the primary source of groundwater replenishment. Since this catchment only has one station that measures rainfall, TRMM rainfall data (Type-3B43-V7) was used to generate rainfall maps in Arc GIS 10.8 using the IDW tool. The rainfall is the second most important factor among the thematic layers with the weight (W) of 0.216 used in this study for creating the GPWZs, as shown in Table 4. The annual precipitation of the research region ranges from 535 to 602 mm, and the rainfall map was classified into five categories as very low potential (rank = 1, class = 535–552), low potential (rank = 3, class = 552–563), moderate potential (rank = 5, class = 563–574), high potential (rank = 7, class = 574–585), and very high potential (rank = 9, class = 585–602), Table 5. Figure 5b, the Sangaw sub-basin rainfall map, shows heavy rainfall in the east and low rainfall in the west.

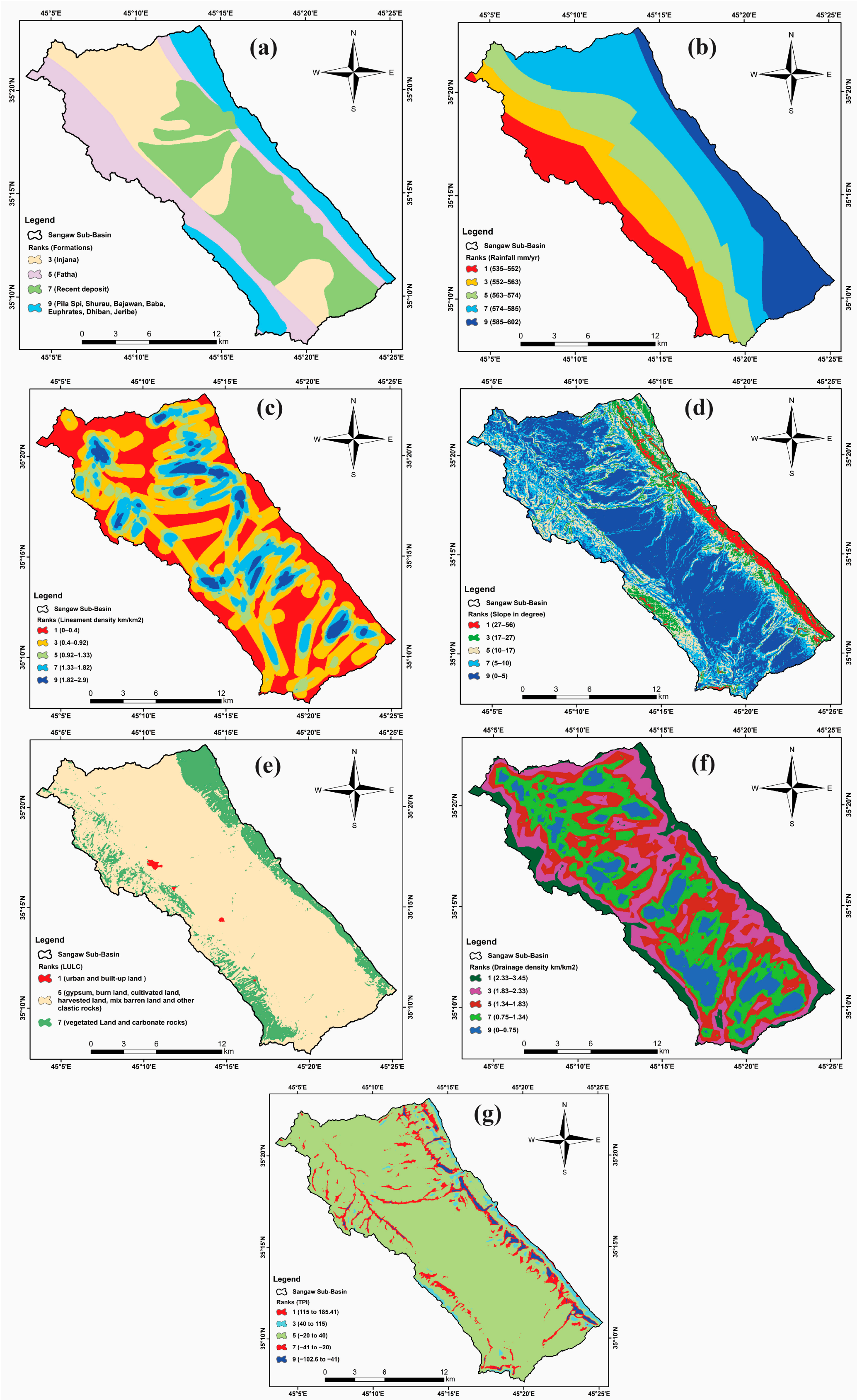

Figure 5. Thematic layers of study region: (**a**) Geology, (**b**) Rainfall, (**c**) Lineament density, (**d**) Slope, (**e**) LULC, (**f**) Drainage density, and (**g**) TPI.

3.1.3. Lineament Density

Lineaments are indicators of fractures and faults in subsurface areas, causing the presence of groundwater to act as canals and reservoirs [82]. Regions with increasing porosity and permeability due to faulting and fracturing are the main indicators of groundwater [83]. The lineament density map of the research area was generated from Landsat 8 Thematic Mapper (TM) images with 30 m spatial resolution. Lineament density occurs in the third order with the weight (W) of 0.129 among the criteria used for generating GWPZs in this study, as demonstrated in Table 4. The lineament density of the research region ranged from 0 to 2.9 km/km^2, and was categorized into five groups. The ranking classes of "1" to "9" as displayed in Figure 5c, cover the study area of 31%, 37%, 14%, 14%, and 4%, respectively.

3.1.4. Slope

The slope is another crucial criterion in determining potential groundwater zones, and can be utilized as an indicator for delineating possible groundwater zones because it regulates the rate of groundwater infiltration. Generally, the infiltration rate is inversely proportional to the slope, and the slope gradient directly controls the infiltration of surface water [72,84]. A steep slope has a low penetration level because the water flows down it rapidly and has inadequate time for infiltration; meanwhile, a flat surface allows rainwater to be retained and helps recharge the groundwater [72,85,86]. The slope map of the Sangaw sub-basin was derived from the STRM DEM 30 m. Slope ranks in the same order as lineament with the weight (W) of 0.129 among the criteria used for generating GWPZs in this study, as displayed in Table 4. The slope of the steady study area was classified into five groups: 0°–5° (very high potential), 5°–10° (high potential), 10°–17° (moderate potential), 17°–27° (low potential), and 27°–56° (very low potential), as shown in Table 5. The rating classes signed with the rate of "1" to "9", as shown in Figure 5d, occupy an area of 4%, 9%, 17%, 25%, and 45% of the research region, respectively.

3.1.5. Land Use/Land Cover

LULC performs a crucial function in recharging groundwater through percolation and leaching [87]. It also gives important information regarding groundwater, infiltration, moisture content, and surface water [79,88]. The study area LULC map, which was provided by the Iraq Geological Survey, was generated using Landsat 8 satellite data, including nine different classes. The weight (W) of LULC is 0.071 among the criteria used for GWPZs delineation of the study area Table 4. The LULC classes were rated with "7" for vegetated Land and carbonate rocks (high potential); "5" for gypsum, burn land, cultivated land, harvested land, mix barren land, and other clastic rocks (moderate potential); "1" for the urban and built-up land (very low potential), as illustrated in Figure 5e. These rating classes occupy 16.1%, 83.6%, and 0.3% of the study area, respectively.

3.1.6. Drainage Density

Drainage density is among the influencing criteria in groundwater potential that impacts runoff and infiltration. A high drainage density means more runoff and less groundwater recharge, whereas a low drainage density implies more groundwater recharge and less runoff [34,70,89]. Drainage density can be defined as the proximity of the distance between stream channels, and it implies the ratio between the total stream length and total area [62,84,90]. The STRM DEM 30 m was used to generate the Sangaw sub-basin drainage density map in ArcGIS software. The drainage density values vary between 0 and 3.45 km/km^2, with the weight (W) of 0.071 among the criteria used for generating GWPZs in the Sangaw sub-basin. The drainage density of the study area was divided into five groups: 0–0.75 km/km^2 (very high potential), 0.75–1.34 km/km^2 (high potential), 1.34–1.83 km/km^2 (moderate potential), 1.83–2.33 km/km^2 (low potential), and 2.33–3.45 km/km^2 (very low potential). Low drainage areas have large weights for the GWPZ delineation, whereas high drainage areas have low weights Table 5. The ratings of these classes range from "1" to "9", as displayed in Figure 5f, covering an area of 13%, 21%, 27%, 27%, and 12% of the study area, respectively.

3.1.7. Topographic Position Index (TPI)

An algorithm called topographic position index (TPI) is broadly used to measure topographic slope positions and automate landform classification [38,91]. The topographic position index is connected with several physical processes that influence the terrain, including hilltop, valley bottom, exposed ridges, flat plain, and upper and lower slope actions [38,92]. TPI is the least important criterion, with the weight (W) of 0.028 used to determine GWPZs of the Sangaw sub-basin in Table 4. The STRM DEM 30 m was used to construct the TPI map of the research region. Positive TPI values demonstrate altitudes that are higher than average, and negative TPI values demonstrate altitudes that are lower than average compared to their surroundings [93,94]. TPI values zero implies a flat ground surface. High TPI values represent upper slopes, whereas low values of TPI indicate lower slopes where the groundwater potential is high [95]. Hence, the high weights are allocated for low TPI while the low weights are allocated for high TPI values. TPI ranges varied from −102.6 to 185.41 in the research region. The TPI of the study area was divided into five groups: −102.6 to −41 (very high potential), −41 to −20 (high potential), −20 to 40 (moderate potential), 40 to 115 (low potential), and 115 to 185.41 (very low potential). The ratings of these classes range from "1" to "9", as shown in Figure 5g, occupying an area of 0.2%, 3.6%, 86.9%, 7.6%, and 1.7% of the study area, respectively.

4. Discussion

4.1. Delineation of GWPZs

Groundwater potential zones are delineated using a combination of GIS, RS, and AHP. The studied area is significantly affected by geology, rainfall, slope, and drainage density in terms of groundwater potential. In regard to importance, geology acquired the highest normalized weight, followed by rainfall, slope, lineament density, LULC, drainage density, and TPI. The map of groundwater potential was generated based on the normalized GWPI values and classified into five classes, namely, very low, low, moderate, high, and very high, as shown in Table 6.

Table 6. Groundwater potential zone derived from AHP.

Class of GWPZs	Area of Coverage (km^2)	Area (%)
Very Low	55.4	14.7
Low	90.4	24
Moderate	68.1	18.1
High	100	26.6
Very High	62.4	16.6

Figure 6 shows the map of GWPZs, which explains the groundwater scenario of the study region. The resulting map displayed almost 39% of the research area covered by very low to low groundwater potential zones because of the distribution of the Fatha and Injana formations (less productive), a small amount of rainfall, and steep slopes, more drainage density, and hilly terrain features around the Ashdagh anticline. Furthermore, the northwestern part and some small patches of the study area are characterized by low to very low groundwater potential zones due to the occurrence of red claystone and grey compact sandstone of the Injana Formation. As can be seen from the GWPZ map, a huge area covers moderate to very high categories, which is around 60% of the Sangaw sub-basin. Moderate groundwater potential zones are spatially distributed over the central part of the study area and along Sagrma mountain, especially where the Fatha Formation is abundant. In addition, this zone is also present in some cultivated land in the central part and areas with less amount of rainfall. High to very high groundwater potential zones are mainly concentrated along the top of Sagrma mountain and in the central part of the study region, where the recent deposit is dominant.

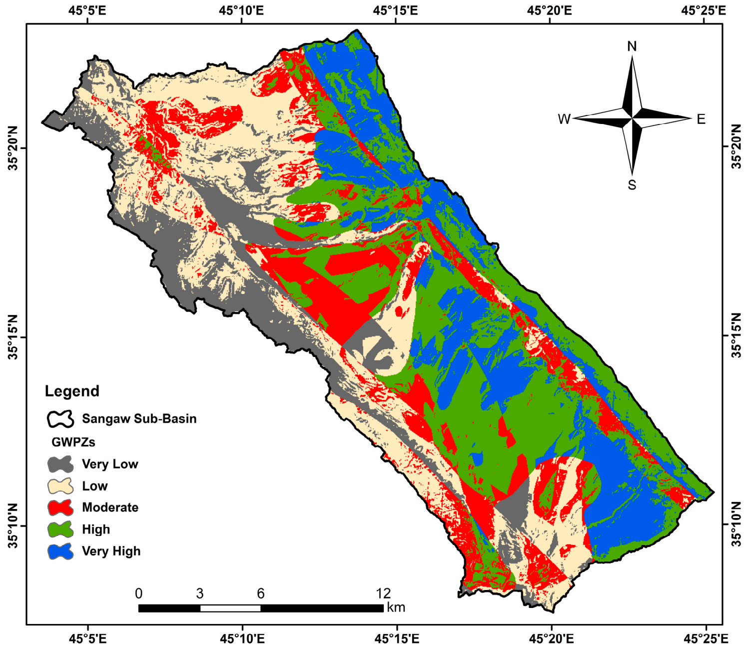

Figure 6. Groundwater potential zones map of Sangaw sub-basin.

In addition, this zone is also present in some cultivated land in the central area and areas with lesser amounts of rainfall. High to very high groundwater potential zones are mainly concentrated along the top of Sagrma mountain and in the central part of the study region, where the recent deposit is dominant. Moreover, the presence of these highly potential zones is mainly due to the distribution of water-bearing and highly fissured rock units, increasing rainfall amount, gentle slope of the central part, agricultural land, and fracture-prone areas. Lastly, the distribution of groundwater is demonstrated to be highly influenced by geology, rainfall, lineament density, drainage density, and TPI on the groundwater potential map.

In terms of data, this study was based on data created mostly by the authors and Iraqi organizations and released to the public; at the same time, it is bound by limitations in data collection, such as water quality. Since the importance of the data used for generating the groundwater potential map is very high, the accuracy of the model will be improved if more data is used in future studies. Finally, groundwater potential studies completely disregard groundwater quality as an important factor in groundwater modelling. The groundwater storage may be large, but its quality is not good, and, thus, the groundwater potential analysis is useless in this case [96]. Due to this, the quality of groundwater should be an important part of the next studies of groundwater potential zones.

4.2. Validation of GWPZs

Validation represents the most crucial step in modeling, since without it, the results have no scientific significance [25,62,97,98]. Groundwater potential validation is usually an expensive and challenging task, especially if the study site is difficult to access in some locations, and if there is a lack of data availability. The challenge is further noticeable in mountainous areas and villages where people use their lands for livestock and agricultural purposes. To verify the results with geospatial data, eight ERT (using Wenner-Schlumberger array) profiles were used to demarcate and validate the GWPZs in the Sangaw sub-basin, as shown in Figure 7.

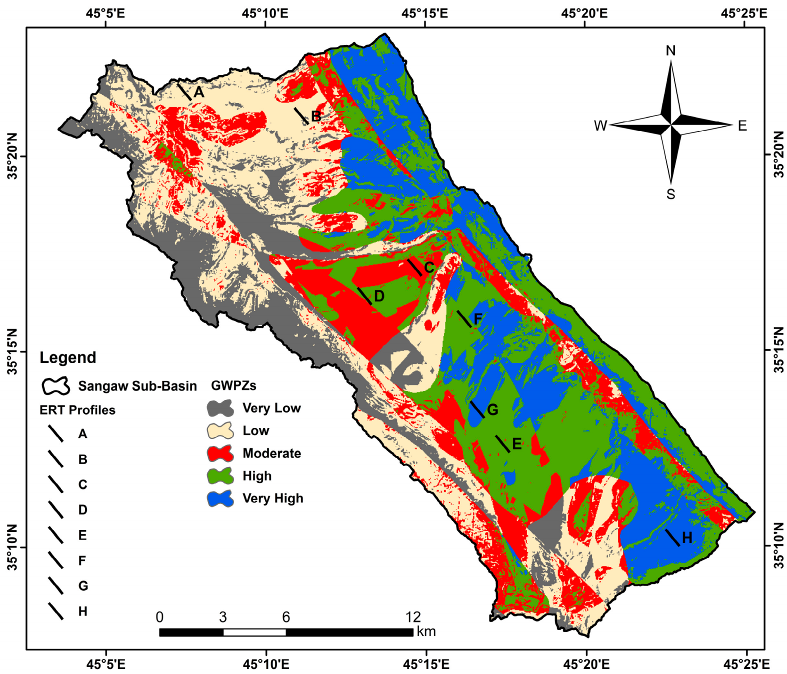

Figure 7. Validation of the GWPZ map showing ERT-profile-lines of Sangaw sub-basin.

The first two profiles, A and B, were chosen in very low to low groundwater potential zones, as displayed in Figure 8a,b. Generally, two distinguished zones have been recognized for each profile; the first zone, which is the thin soil covered zone (weathered zone), is composed of less productive material of the Injana Formation (clay, silt, and dry sand), whereas the second zone, which is depicted by the dark blue color, is completely composed of claystone with little siltstone. In terms of thickness, lithology, and resistivity of the indicated zones, both profiles are quite similar. The first zone is recognized by an average thickness of about 10 m, and a relatively low resistivity value ranging from 20 Ωm to 60 Ωm; whereas the second zone of silty claystone is approximately 140 m thick, and has a very low resistivity value of 7.1 Ωm to 15 Ωm. As a result, these sites cannot be recommended for groundwater investigation due to the very little quantity of water, which would not be sufficient for even short-term sustainability.

The 2D resistivity profiles C and D were selected in moderate and moderate-to-high GWPZs, respectively, as shown in Figure 8c,d. The inverse section of profile C shows the existence of a moderate resistive recent deposit (20–170 Ωm). It has a thickness ranging from 3 m to 40 m, and is mainly composed of clay, silt, sand, and some limestone fragments of the Pila Spi Formation. Alternation of thick claystone, silty sandstone, and sandstone layers of the Injana Formation occur directly beneath the recent deposit, it has a low resistivity value from 7.35 Ωm to 35 Ωm. This site is generally considered a moderate GWPZs due to the existence of relatively thick recent sediments. The 2D results of profile D show that the section includes three distinct zones. The upper zone has low resistivity, ranging from 7.5 Ωm to 50 Ωm, with an average thickness of 10 m, indicating a water-bearing weathered zone. The middle zone indicates high GWPZs especially from electrodes 1–44 due to the presence of a 30 m sandstone bed; whereas electrodes 44–72 show moderate GWPZs, due to the existence of silt materials. The lower zone has very low resistivity, indicating silty claystone, which makes the zone much less productive for GWPZs.

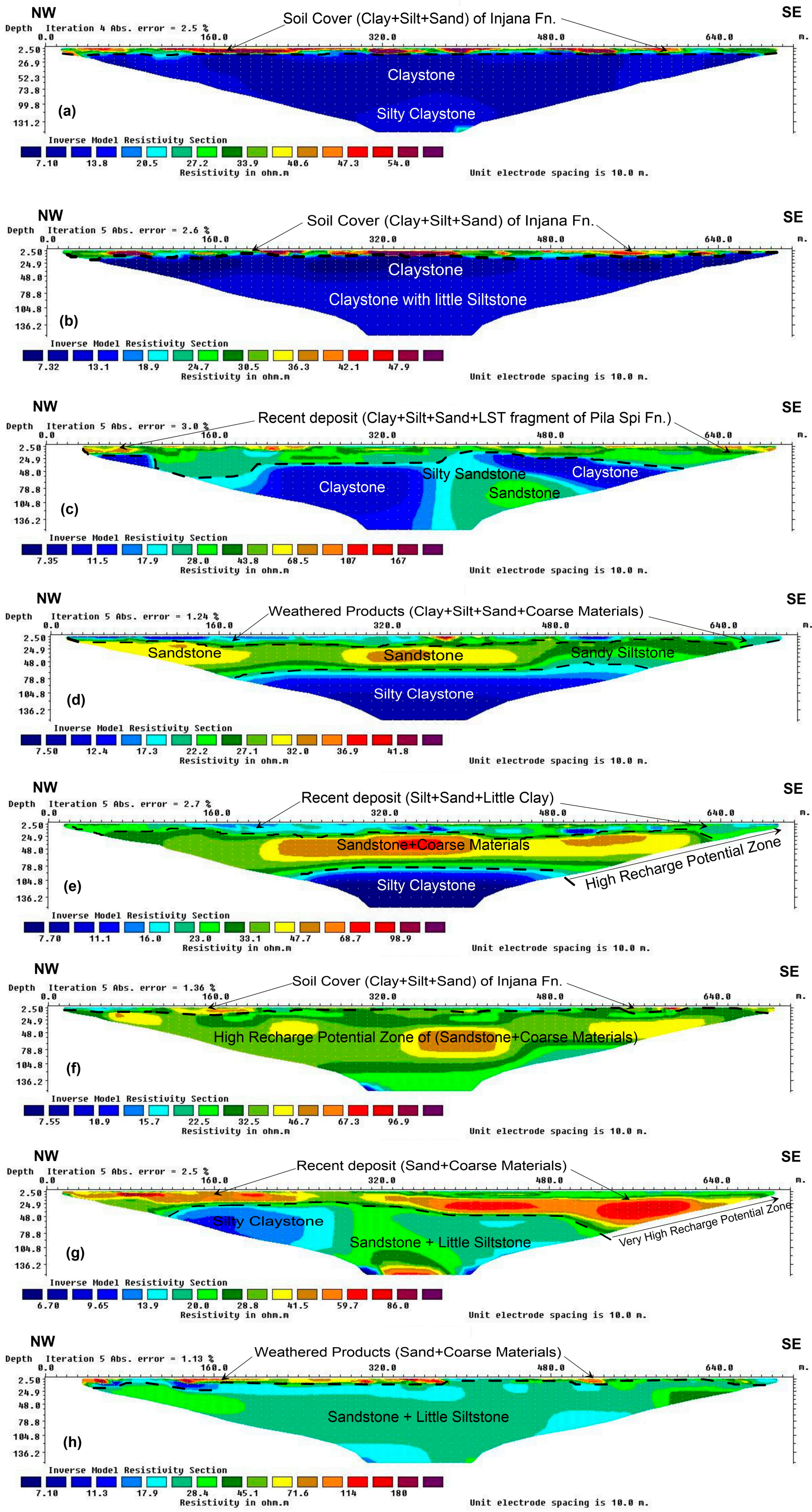

Figure 8. Resistivity inversion profiles in the Sangaw sub-basin. (**a**,**b**) low to very low, (**c**) moderate, (**d**) moderate to high, (**e**,**f**) high, and (**g**,**h**) very high groundwater potential zones.

The 2D ERT profiles of E and F were chosen in high groundwater potential zones as illustrated in Figure 8e,f. The inverse section of profile E shows three separate zones. The upper zone has low resistivity, ranging from 7.7 Ωm to 33 Ωm, with an average thickness of about 20 m, showing a water-bearing zone of the recent deposit. The middle zone shows high GWPZs, especially from electrodes 20–62, due to the presence of about 60 m of sandstone and coarse materials, with a resistivity value ranging from 30 Ωm to 100 Ωm. The lower zone is characterized by the existence of silty claystone, which is approximately 70 m thick, and has a very low resistivity value of 7.7 Ωm to 20 Ωm. The 2D resistivity section of profile F includes two distinguished zones. The upper zone, which is approximately 4 m thin solid cover zone, is composed of silt, sand, and coarse materials with a resistivity value ranging from 20 Ωm to 50 Ωm. The lower zone shows that the subsurface of this site mainly consists of sandstone, coarse material. In addition, the high GWPZ of sandstone and coarse material of recent deposit is dominant, and has a low resistivity value ranging from 25 Ωm to 70 Ωm, which leads to the area having more productivity for GWPZs.

The last two profiles, G and H, were conducted in a very high groundwater potential zone, as shown in Figure 8g,h. As can be seen from profile G, the near surface of this zone is described by the presence of sand and coarse materials with a resistivity value of 20–100 Ωm, which leads to the zone having more products for GWPZs. A layer of claystone and silty sandstone of the Injana Formation occurs directly beneath this zone, which makes the zone relatively less water-bearing compared with the near-surface zone. As can be observed from profile H, the results of the 2D resistivity section include two distinct zones. The first zone is a thin weathered product zone of sand, coarse material, and a product of clay, which has various resistivity values ranging from 7 Ωm to 100 Ωm as a result of the different lithological compositions and the level of weathering of rocks. Thick sandstone and little siltstone layers, which have a resistivity value of about 20–45 Ωm, occur directly beneath the first zone and extend to the maximum depth of investigation, which is equal to 150 m. Furthermore, the moderate resistivity values, high thickness (more than 100 m), and lithological properties of these two profiles showed that the very high GWPZs of the study area had good groundwater availability, which is in line with the groundwater potential map.

Generally, the 2D electrical resistivity tomography (ERT) technique supported the groundwater development prospective model, which provides the map of groundwater potential with a high level of validity and confidence. Finally, the validation of GWPZs reveals that the model offers future recommendations for developing appropriate groundwater exploration strategies and plans.

5. Conclusions

In this study, groundwater potential zones have been defined using a combined approach of GIS and multi-criteria decision analysis (MCDA) for the Sangaw sub-basin. The AHP technique was chosen for the MCDA between the main thematic layers (and their features/classes) influencing the groundwater potential of the study area. As the main themes, geology, rainfall, slope, lineament density, drainage density, LULC, and topographic position index layers were chosen, appraised, and explicated. The thematic layers were allocated different ranks and their classes obtained different weights according to their influence on groundwater potential. The weights and ranks were allocated according to the author's knowledge, field observations, and relevant studies. Consequently, after integrating all the thematic maps into the ArcGIS 10.8 software, a groundwater potential map was generated for the research area.

The GWPZs map was categorized into five classes: very high (62.4 km^2), high (100 km^2), moderate (68.1 km^2), low (90.4 km^2), and very low (55.4 km^2). The most favorable zone for groundwater prospects is the very high zone, whereas the least favorable zone is the very low zone. The very high and high GWPZs are mostly situated along the top of Sagrma mountain and in the middle part of the research area, and cover 16.6% and 26.6%, respectively, of the entire region. Moderate GWPZs, which are spread over the study area, cover an area of about 18.1%. Very low and low GWPZs are mainly located in the northwest part, where the Fatha and Injana Formations are dominant, and around the Ashdagh anticline, covering 14.7% and 24% of the total area, respectively. Overall, the findings demonstrate that geology and rainfall mainly influence the distribution of groundwater in the Sangaw sub-basin.

The validation was carried out by conducting a 2D ERT survey at eight locations to comprehend the groundwater scenario of the area, which displays an excellent agreement with the GWPZs map results. The outcomes of profiles A and B, which are located in very low to low GWPZs, indicate that the area lacks adequate groundwater supplies. The results of profiles C and D show moderate and moderate-to-high GWPZs, respectively. The 2D inverse sections of profiles E and F show high GWPZs, whereas the sections of profiles G and H indicate very high GWPZs. Additionally, validation with ERT has been demonstrated to be effective for assessing groundwater potential in areas with a lack of data. Furthermore, the overall outcomes and results of this study are very beneficial for the exploration and development of groundwater resources for local people and policymakers in the Sangaw sub-basin.

Finally, the study of groundwater potential should consider groundwater quality as a crucial factor. If groundwater storage is large, but its quality is poor, the groundwater potential mapping analysis is useless. Moreover, groundwater recharge estimation using the newest techniques is essential for sustainable water management and water supply schemes in future studies.

Author Contributions: The first author, A.S., proposed the topic and spearheaded the data processing and analysis, and the writing of the manuscript because this is a part of his Ph.D. thesis. D.A.M.A.-M. and B.Q.A.: They helped to edit the manuscript as they are supervisors of the first author. All authors have read and agreed to the published version of the manuscript.

Funding: No funding was received for conducting this study.

Institutional Review Board Statement: Not applicable.

Informed Consent Statement: Not applicable.

Data Availability Statement: Not applicable.

Acknowledgments: This research is a section of the first author's Ph.D. thesis. The authors acknowledge the Geology Department, University of Sulaimani, for supplying the necessary geophysical equipment to conduct this research, and the Sangaw Agricultural Directorate for their kind assistance in providing the available rainfall data. Special thanks to all our colleagues, Hawber A., Hemn F., and Assad I. Zana M., for assisting in the field data acquisition. Great appreciation goes to Arsalan Ahmed Othman for his continuous support in applying the ArcGIS technique.

Conflicts of Interest: The authors declare that they have no competing interests.

References

1. Mogaji, K.A.; Lim, H.S.; Abdullah, K. Regional Prediction of Groundwater Potential Mapping in a Multifaceted Geology Terrain Using GIS-Based Dempster–Shafer Model. *Arab. J. Geosci.* **2015**, *8*, 3235–3258. [CrossRef]
2. Todd, D.K.; Mays, L.W. *Groundwater Hydrology*, 3rd ed.; John Wiley and Sons, Inc.: Hoboken, NJ, USA, 2005.
3. Pandey, K.; Kumar, S.; Malik, A.; Kuriqi, A. Artificial Neural Network Optimized with a Genetic Algorithm for Seasonal Groundwater Table Depth Prediction in Uttar Pradesh, India. *Sustainability* **2020**, *12*, 8932. [CrossRef]
4. Jha, M.K.; Chowdary, V.M.; Chowdhury, A. Groundwater Assessment in Salboni Block, West Bengal (India) Using Remote Sensing, Geographical Information System and Multi-Criteria Decision Analysis Techniques. *Hydrogeol. J.* **2010**, *18*, 1713–1728. [CrossRef]
5. Foster, S.S.D.; Chilton, P.J. Groundwater: The Processes and Global Significance of Aquifer Degradation. *Philos. Trans. R. Soc. London. Ser. B Biol. Sci.* **2003**, *358*, 1957–1972. [CrossRef] [PubMed]
6. Nivesh, S.; Patil, J.P.; Goyal, V.C.; Saran, B.; Singh, A.K.; Raizada, A.; Malik, A.; Kuriqi, A. Assessment of Future Water Demand and Supply Using WEAP Model in Dhasan River Basin, Madhya Pradesh, India. *Environ. Sci. Pollut. Res.* **2022**, 1–14. [CrossRef]
7. Khafaji, M.S.A.; Alwan, I.A.; Khalaf, A.G.; Bhat, S.A.; Kuriqi, A. Potential Use of Groundwater for Irrigation Purposes in the Middle Euphrates Region, Iraq. *Sustain. Water Resour. Manag.* **2022**, *8*, 157. [CrossRef]

8. Kuriqi, A.; Ali, R.; Pham, Q.B.; Gambini, J.M.; Gupta, V.; Malik, A.; Linh, N.T.T.; Joshi, Y.; Anh, D.T.; Nam, V.T.; et al. Seasonality shift and streamflow flow variability trends in central India. *Acta Geophys.* **2020**, *68*, 1461–1475. [CrossRef]
9. Kuriqi, A.; Pinheiro, A.N.; Sordo-Ward, A.; Garrote, L. Water-Energy-Ecosystem Nexus: Balancing Competing Interests at a Run-of-River Hydropower Plant Coupling a Hydrologic–Ecohydraulic Approach. *Energy Convers. Manag.* **2020**, *223*, 113267. [CrossRef]
10. Bastani, M.; Kholghi, M.; Rakhshandehroo, G.R. Inverse Modeling of Variable-Density Groundwater Flow in a Semi-Arid Area in Iran Using a Genetic Algorithm. *Hydrogeol. J.* **2010**, *18*, 1191–1203. [CrossRef]
11. Arkoprovo, B.; Adarsa, J.; Prakash, S.S. Delineation of Groundwater Potential Zones Using Satellite Remote Sensing and Geographic Information System Techniques: A Case Study from Ganjam District, Orissa, India. *Res. J. Recent Sci.* **2012**, *1*, 59–66.
12. Lee, G.F.; Jones-Lee, A. Evaluation of Surface Water Quality Impacts of Hazardous Chemical Sites. *Remediat. J.* **1999**, *9*, 87–113. [CrossRef]
13. Simeonov, V.; Stratis, J.A.; Samara, C.; Zachariadis, G.; Voutsa, D.; Anthemidis, A.; Sofoniou, M.; Kouimtzis, T. Assessment of the Surface Water Quality in Northern Greece. *Water Res.* **2003**, *37*, 4119–4124. [CrossRef] [PubMed]
14. Maity, D.K.; Mandal, S. Identification of Groundwater Potential Zones of the Kumari River Basin, India: An RS & GIS Based Semi-Quantitative Approach. *Environ. Dev. Sustain.* **2019**, *21*, 1013–1034.
15. Ozdemir, A. GIS-Based Groundwater Spring Potential Mapping in the Sultan Mountains (Konya, Turkey) Using Frequency Ratio, Weights of Evidence and Logistic Regression Methods and Their Comparison. *J. Hydrol.* **2011**, *411*, 290–308. [CrossRef]
16. Madani, A.; Niyazi, B. Groundwater Potential Mapping Using Remote Sensing Techniques and Weights of Evidence GIS Model: A Case Study from Wadi Yalamlam Basin, Makkah Province, Western Saudi Arabia. *Environ. Earth Sci.* **2015**, *74*, 5129–5142. [CrossRef]
17. Park, S.; Hamm, S.-Y.; Jeon, H.-T.; Kim, J. Evaluation of Logistic Regression and Multivariate Adaptive Regression Spline Models for Groundwater Potential Mapping Using R and GIS. *Sustainability* **2017**, *9*, 1157. [CrossRef]
18. Miraki, S.; Zanganeh, S.H.; Chapi, K.; Singh, V.P.; Shirzadi, A.; Shahabi, H.; Pham, B.T. Mapping Groundwater Potential Using a Novel Hybrid Intelligence Approach. *Water Resour. Manag.* **2019**, *33*, 281–302. [CrossRef]
19. Lee, S.; Hong, S.-M.; Jung, H.-S. GIS-Based Groundwater Potential Mapping Using Artificial Neural Network and Support Vector Machine Models: The Case of Boryeong City in Korea. *Geocarto Int.* **2018**, *33*, 847–861. [CrossRef]
20. Naghibi, S.A.; Pourghasemi, H.R. A Comparative Assessment between Three Machine Learning Models and Their Performance Comparison by Bivariate and Multivariate Statistical Methods in Groundwater Potential Mapping. *Water Resour. Manag.* **2015**, *29*, 5217–5236. [CrossRef]
21. Naghibi, S.A.; Pourghasemi, H.R.; Dixon, B. GIS-Based Groundwater Potential Mapping Using Boosted Regression Tree, Classification and Regression Tree, and Random Forest Machine Learning Models in Iran. *Environ. Monit. Assess.* **2016**, *188*, 1–27. [CrossRef]
22. Naghibi, S.A.; Pourghasemi, H.R.; Abbaspour, K. A comparison between ten advanced and soft computing models for groundwater qanat potential assessment in Iran using R and GIS. *Theor. Appl. Clim.* **2018**, *131*, 967–984. [CrossRef]
23. Madrucci, V.; Taioli, F.; de Araújo, C.C. Groundwater Favorability Map Using GIS Multicriteria Data Analysis on Crystalline Terrain, Sao Paulo State, Brazil. *J. Hydrol.* **2008**, *357*, 153–173. [CrossRef]
24. Pietersen, K. Multiple Criteria Decision Analysis (MCDA): A Tool to Support Sustainable Management of Groundwater Resources in South Africa. *Water SA* **2006**, *32*, 119–128. [CrossRef]
25. Rahmati, O.; Nazari Samani, A.; Mahdavi, M.; Pourghasemi, H.R.; Zeinivand, H. Groundwater Potential Mapping at Kurdistan Region of Iran Using Analytic Hierarchy Process and GIS. *Arab. J. Geosci.* **2015**, *8*, 7059–7071. [CrossRef]
26. Saaty, T.L. *The Analytical Hierarchy Process: Planning, Priority Setting, Resources Allocation*; McGraw-Hill: New York, NY, USA, 1980.
27. Chowdhury, A.; Jha, M.K.; Chowdary, V.M. Delineation of Groundwater Recharge Zones and Identification of Artificial Recharge Sites in West Medinipur District, West Bengal, Using RS, GIS and MCDM Techniques. *Environ. Earth Sci.* **2010**, *59*, 1209–1222. [CrossRef]
28. Hajkowicz, S.; Higgins, A. A Comparison of Multiple Criteria Analysis Techniques for Water Resource Management. *Eur. J. Oper. Res.* **2008**, *184*, 255–265. [CrossRef]
29. Kaliraj, S.; Chandrasekar, N.; Magesh, N.S. Identification of Potential Groundwater Recharge Zones in Vaigai Upper Basin, Tamil Nadu, Using GIS-Based Analytical Hierarchical Process (AHP) Technique. *Arab. J. Geosci.* **2014**, *7*, 1385–1401. [CrossRef]
30. Murthy, K.S.R.; Mamo, A.G. Multi-criteria Decision Evaluation in Groundwater Zones Identification in Moyale-Teltele Subbasin, South Ethiopia. *Int. J. Remote Sens.* **2009**, *30*, 2729–2740. [CrossRef]
31. Hajkowicz, S.; Collins, K. A Review of Multiple Criteria Analysis for Water Resource Planning and Management. *Water Resour. Manag.* **2007**, *21*, 1553–1566. [CrossRef]
32. Chenini, I.; Mammou, A.B.; El May, M. Groundwater Recharge Zone Mapping Using GIS-Based Multi-Criteria Analysis: A Case Study in Central Tunisia (Maknassy Basin). *Water Resour. Manag.* **2010**, *24*, 921–939. [CrossRef]
33. Andualem, T.G.; Demeke, G.G. Groundwater potential assessment using GIS and remote sensing: A case study of Guna tana landscape, upper blue Nile Basin, Ethiopia. *J. Hydrol. Reg. Stud.* **2019**, *24*, 100610. [CrossRef]
34. Das, B.; Pal, S.C.; Malik, S.; Chakrabortty, R. Modeling groundwater potential zones of Puruliya district, West Bengal, India using remote sensing and GIS techniques. *Geol. Ecol. Landscapes* **2019**, *3*, 223–237. [CrossRef]

35. Jha, M.K.; Chowdhury, A.; Chowdary, V.M.; Peiffer, S. Groundwater Management and Development by Integrated Remote Sensing and Geographic Information Systems: Prospects and Constraints. *Water Resour. Manag.* **2007**, *21*, 427–467. [CrossRef]
36. Kaur, L.; Rishi, M.S.; Singh, G.; Thakur, S.N. Groundwater Potential Assessment of an Alluvial Aquifer in Yamuna Sub-Basin (Panipat Region) Using Remote Sensing and GIS Techniques in Conjunction with Analytical Hierarchy Process (AHP) and Catastrophe Theory (CT). *Ecol. Indic.* **2020**, *110*, 105850. [CrossRef]
37. Shahid, S.; Nath, S.K.; Roy, J. Groundwater potential modelling in a soft rock area using a GIS. *Int. J. Remote. Sens.* **2000**, *21*, 1919–1924. [CrossRef]
38. Arulbalaji, P.; Padmalal, D.; Sreelash, K. GIS and AHP Techniques Based Delineation of Groundwater Potential Zones: A Case Study from Southern Western Ghats, India. *Sci. Rep.* **2019**, *9*, 1–17. [CrossRef] [PubMed]
39. Kumar, D.; Mondal, S.; Warsi, T. Deep Insight to the Complex Aquifer and Its Characteristics from High Resolution Electrical Resistivity Tomography and Borehole Studies for Groundwater Exploration and Development. *J. Earth Syst. Sci.* **2020**, *129*, 1–15. [CrossRef]
40. Chowdary, V.M.; Chakraborthy, D.; Jeyaram, A.; Murthy, Y.V.N.; Sharma, J.R.; Dadhwal, V.K. Multi-Criteria Decision Making Approach for Watershed Prioritization Using Analytic Hierarchy Process Technique and GIS. *Water Resour. Manag.* **2013**, *27*, 3555–3571. [CrossRef]
41. Al-Manmi, D.A.M.; Rauf, L.F. Groundwater Potential Mapping Using Remote Sensing and GIS-Based, in Halabja City, Kurdistan, Iraq. *Arab. J. Geosci.* **2016**, *9*, 357. [CrossRef]
42. Islami, N.; Taib, S.H.; Yusoff, I.; Ghani, A.A. Integrated geoelectrical resistivity and hydrogeochemical methods for delineating and mapping heavy metal zone in aquifer system. *Environ. Earth Sci.* **2018**, *77*, 383. [CrossRef]
43. Karim, H.A.; Al-Manmi, D.A. Integrating GIS-Based and Geophysical Techniques for Groundwater Potential Assessment in Halabja Said Sadiq Sub-Basin, Kurdistan, NE Iraq. *Tikrit J. Pure Sci.* **2019**, *24*, 81–92. [CrossRef]
44. Mogaji, K.A.; Omosuyi, G.O.; Adelusi, A.O.; Lim, H.S. Application of GIS-Based Evidential Belief Function Model to Regional Groundwater Recharge Potential Zones Mapping in Hardrock Geologic Terrain. *Environ. Process.* **2016**, *3*, 93–123. [CrossRef]
45. Mohammed, S. Groundwater Potential Mapping Using Remote Sensing and GIS of a Part of Chamchamal Basin, Sulaimani, Kurdistan Region, Iraq. Master's Thesis, University of Miskolc, Miskolc, Hungary, 2017; 70p.
46. Oh, H.-J.; Kim, Y.-S.; Choi, J.-K.; Park, E.; Lee, S. GIS Mapping of Regional Probabilistic Groundwater Potential in the Area of Pohang City, Korea. *J. Hydrol.* **2011**, *399*, 158–172. [CrossRef]
47. Sonkamble, S.; Satishkumar, V.; Amarender, B.; Sethurama, S. Combined Ground-Penetrating Radar (GPR) and Electrical Resistivity Applications Exploring Groundwater Potential Zones in Granitic Terrain. *Arab. J. Geosci.* **2014**, *7*, 3109–3117. [CrossRef]
48. Venkateswaran, S.; Prabhu, M.V.; Karuppannan, S. Delineation of Groundwater Potential Zones Using Geophysical and GIS Techniques in the Sarabanga Sub Basin, Cauvery River, Tamil Nadu, India. *Int. J. Curr. Res. Acad. Rev.* **2014**, *2*, 58–75.
49. Kowalsky, M.B.; Gasperikova, E.; Finsterle, S.; Watson, D.; Baker, G.; Hubbard, S.S. Coupled Modeling of Hydrogeochemical and Electrical Resistivity Data for Exploring the Impact of Recharge on Subsurface Contamination. *Water Resour. Res.* **2011**, *47*, 1–22. [CrossRef]
50. Al-Manmi, D.A.M.A.; Ismaeel, S.B.; Altaweel, M. Reconstruction of palaeoclimate in Shalaii Cave, SE of Sangaw, Kurdistan Province of Iraq. *Palaeogeogr. Palaeoclim. Palaeoecol.* **2019**, *524*, 262–272. [CrossRef]
51. Iurkiewicz, A.A.; Stevanovic, Z.P. Reconnaissance Study of Active Sulfide Springs and Cave Systems in the Southern Part of the Sulaimani Governorate (NE Iraq). *Carbonates Evaporites* **2010**, *25*, 203–216. [CrossRef]
52. Othman, A.A.; Shihab, A.T.; Al-Maamar, A.F.; Al-Saady, Y.I. Monitoring of the Land Cover Changes in Iraq. In *Environmental Remote Sensing and GIS in Iraq*; Springer: Berlin/Heidelberg, Germany, 2020; pp. 181–203.
53. Abdullah, H.G.; Collier, R.E.L.; Mountney, N.P. The palaeoshoreline of Early Miocene formations (Euphrates and Jeribe) at the periphery of the Zagros Foreland Basin, Sulaimani Governorate, Kurdistan Region, NE Iraq. *Arab. J. Geosci.* **2019**, *12*, 574. [CrossRef]
54. Jassim, S.Z.; Goff, J.C. *Geology of Iraq*; DOLIN, sro, distributed by Geological Society of London: London, UK, 2006; ISBN 8070282878.
55. Khanaqa, P.A.; Karim, K.H. Stratigraphical and Structural Analyses of the Sagrma (Sagerma) Anticline, Sulaimani Area, Iraqi Kurdistan Region. *J. Geogr. Geol.* **2015**, *7*, 74. [CrossRef]
56. Kharajiany, S.O. The Occurrence of Early and Middle Miocene Rocks (Euphrates, Dhiban and Jeribe Formations) In Ashdagh Mountain, Sangaw Area, Sulaimaniyah Vicinity, NE Iraq. *Iraqi Bull. Geol. Min.* **2014**, *10*, 21–39.
57. Kharajiany, S.O.A. Sedimentary Facies of Oligocene Rock Units in Ashdagh Mountain-Sangaw District-Kurdistan Region. Master's Thesis, University of Sulaimani, Sulaimani, Iraq, 2008.
58. Al-Manmi, D.A.M.; Aziz, B.Q.; Kareem, A.T.; Othman, H.A.; Mohammed, S.H.; Karim, H.A.; Mustafa, A.I.; Muhammed, H.F. A Study of Mineralized Water Using Geophysical and Hydrogeochemical Approaches in Khwelen Salt Ponds, Sangaw, Sulaymaniyah, NE of Iraq. *Tikrit J. Pure Sci.* **2021**, *25*, 47–61.
59. Stevanovic, Z.; Markovic, M. *Hydrogeology of Northern Iraq. Vol. 1. Climate, Hydrology, Geomorphology & Geology. Vol. 2. General Hydrogeology and Aquifer Systems*; FAO: Rome, Italy, 2004.
60. Al-Hafeed, S.B.I. *Reconstructing of Paleoclimate through Hydrogeological and Environmental Studies of Shalaii Cave, SE of Sangaw, Iraqi Kurdistan Region, Sulaimani*; University of Sulaimani: Sulaimani, Iraq, 2016.

61. Patra, S.; Mishra, P.; Mahapatra, S.C. Delineation of Groundwater Potential Zone for Sustainable Development: A Case Study from Ganga Alluvial Plain Covering Hooghly District of India Using Remote Sensing, Geographic Information System and Analytic Hierarchy Process. *J. Clean. Prod.* **2018**, *172*, 2485–2502. [CrossRef]
62. Pathmanandakumar, V.; Thasarathan, N.; Ranagalage, M. An Approach to Delineate Potential Groundwater Zones in Kilinochchi District, Sri Lanka, Using GIS Techniques. *ISPRS Int. J. Geo-Inf.* **2021**, *10*, 730. [CrossRef]
63. Ma'ala, K.A. The Geology of Sulaimaniya Quadrangle. Sheet No. Ni-38–3, Scale 1: 250000. *Geol. Surv. Iraq* **2008**, *80*.
64. Sissakian, V.; Geologist, E.P.C.; Fouad, S.F.; General, I.G.S.D. Geological map of Sulaimaniyah quadrangle, at scale of 1: 250,000. *J. Zankoy Sulaimani—Part A* **2014**, *GeoKurdist*, 151–161. [CrossRef]
65. GSFC_DAAC Tropical Rainfall Measurement Mission Project (TRMM; 3B43 V7). Available online: https://disc.gsfc.nasa.gov/datasets/TRMM_3B43_7/summary (accessed on 21 January 2023).
66. Al-Rubaiay, A.T.; Al-Dulaimi, T.Y. Series of Land Use Land Cover Maps of Iraq Scale 1: 250 000. *Sulaimaniya Quadrang. Sheet NI–38–3 (LULCM 10)*. 2012. Available online: http://iiir-mim.gov.iq/xmlui/handle/123456789/32976 (accessed on 7 November 2022).
67. Saaty, T. A scaling method for priorities in hierarchical structures. *J. Math. Psychol.* **1977**, *15*, 234–281. [CrossRef]
68. Rajasekhar, M.; Raju, G.S.; Sreenivasulu, Y.; Raju, R.S. Delineation of Groundwater Potential Zones in Semi-Arid Region of Jilledubanderu River Basin, Anantapur District, Andhra Pradesh, India Using Fuzzy Logic, AHP and Integrated Fuzzy-AHP Approaches. *HydroResearch* **2019**, *2*, 97–108. [CrossRef]
69. Saaty, T.L. *Decision Making for Leaders: The Analytic Hierarchy Process for Decisions in a Complex World*; RWS publications: Pittsburgh, PA, USA, 1990; ISBN 1888603135.
70. Ahmadi, H.; Kaya, O.A.; Babadagi, E.; Savas, T.; Pekkan, E. GIS-Based Groundwater Potentiality Mapping Using AHP and FR Models in Central Antalya, Turkey. *Environ. Sci. Proc.* **2020**, *5*, 11.
71. Kumari, A.; Kumar, D.; Warwade, P. Application of Multi-Criteria Decision Making (MCDM) and Electrical Resistivity Tomography (ERT) Techniques for Identification of Groundwater Recharge Zone(s) in Granitic Hard Rock Aquifer. *J. Earth Syst. Sci.* **2021**, *130*, 1–17. [CrossRef]
72. Kumar, V.A.; Mondal, N.C.; Ahmed, S. Identification of Groundwater Potential Zones Using RS, GIS and AHP Techniques: A Case Study in a Part of Deccan Volcanic Province (DVP), Maharashtra, India. *J. Indian Soc. Remote. Sens.* **2020**, *48*, 497–511. [CrossRef]
73. Sapkota, S.; Pandey, V.P.; Bhattarai, U.; Panday, S.; Shrestha, S.R.; Maharjan, S.B. Groundwater potential assessment using an integrated AHP-driven geospatial and field exploration approach applied to a hard-rock aquifer Himalayan watershed. *J. Hydrol. Reg. Stud.* **2021**, *37*, 100914. [CrossRef]
74. Aziz, B.Q. Two Dimension Resistivity Imaging Tomography for Hydrogeological Study in Bazian Basin, West Sulaimani City, NE-Iraq. Ph. D. Thesis, University of Sulaimani, Sulaymaniyah, Iraq, 2005.
75. Loke, M.H. *Rapid 2-D Resistivity & IP Inversion Using the Least-Squares Method*; Geoelectrical Imaging 2D & 3D; Geotomo Software: Penang, Malaysia, 2007.
76. Loke, M.H.; Barker, R.D. Rapid Least-squares Inversion of Apparent Resistivity Pseudosections by a Quasi-Newton Method1. *Geophys. Prospect.* **1996**, *44*, 131–152. [CrossRef]
77. Dahlin, T. 2D resistivity surveying for environmental and engineering applications. *First Break.* **1996**, *14*, 275–283. [CrossRef]
78. Loke, M.H. Electrical Imaging Surveys for Environmental and Engineering Studies. *Pract. Guide* **1999**, *2*, 70.
79. Bhunia, G.S. An Approach to Demarcate Groundwater Recharge Potential Zone Using Geospatial Technology. *Appl. Water Sci.* **2020**, *10*, 138. [CrossRef]
80. Adiat, K.; Nawawi, M.; Abdullah, K. Assessing the accuracy of GIS-based elementary multi criteria decision analysis as a spatial prediction tool—A case of predicting potential zones of sustainable groundwater resources. *J. Hydrol.* **2012**, *440-441*, 75–89. [CrossRef]
81. Razandi, Y.; Pourghasemi, H.R.; Neisani, N.S.; Rahmati, O. Application of Analytical Hierarchy Process, Frequency Ratio, and Certainty Factor Models for Groundwater Potential Mapping Using GIS. *Earth Sci. Inform.* **2015**, *8*, 867–883. [CrossRef]
82. Ahirwar, S.; Malik, M.S.; Ahirwar, R.; Shukla, J.P. Application of Remote Sensing and GIS for Groundwater Recharge Potential Zone Mapping in Upper Betwa Watershed. *J. Geol. Soc. India* **2020**, *95*, 308–314. [CrossRef]
83. Das, S.; Gupta, A.; Ghosh, S. Exploring Groundwater Potential Zones Using MIF Technique in Semi-Arid Region: A Case Study of Hingoli District, Maharashtra. *Spat. Inf. Res.* **2017**, *25*, 749–756. [CrossRef]
84. Ibrahim-Bathis, K.; Ahmed, S. Geospatial technology for delineating groundwater potential zones in Doddahalla watershed of Chitradurga district, India. *Egypt. J. Remote. Sens. Space Sci.* **2016**, *19*, 223–234. [CrossRef]
85. Senarathne, S.L.; Jayawardana, J.; Edirisinghe, E.; Chandrajith, R. Characterization of Groundwater in Malala Oya River Basin, Sri Lanka Using Geochemical and Isotope Signatures. *Groundw. Sustain. Dev.* **2019**, *9*, 100225. [CrossRef]
86. Das, B.; Pal, S.C. Combination of GIS and Fuzzy-AHP for Delineating Groundwater Recharge Potential Zones in the Critical Goghat-II Block of West Bengal, India. *HydroResearch* **2019**, *2*, 21–30. [CrossRef]
87. Sarwar, A.; Ahmad, S.; Rehmani, M.; Javid, M.A.; Gulzar, S.; Shehzad, M.; Dar, J.S.; Baazeem, A.; Iqbal, M.; Rahman, M.; et al. Mapping Groundwater Potential for Irrigation, by Geographical Information System and Remote Sensing Techniques: A Case Study of District Lower Dir, Pakistan. *Atmosphere* **2021**, *12*, 669. [CrossRef]
88. Anderson, G.B.; Barnes, E.A.; Bell, M.L.; Dominici, F. The Future of Climate Epidemiology: Opportunities for Advancing Health Research in the Context of Climate Change. *Am. J. Epidemiol.* **2019**, *188*, 866–872. [CrossRef] [PubMed]

89. Saha, D.; Dhar, Y.R.; Vittala, S.S. Delineation of Groundwater Development Potential Zones in Parts of Marginal Ganga Alluvial Plain in South Bihar, Eastern India. *Environ. Monit. Assess.* **2010**, *165*, 179–191. [CrossRef]
90. Chakrabortty, R.; Pal, S.C.; Malik, S.; Das, B. Modeling and Mapping of Groundwater Potentiality Zones Using AHP and GIS Technique: A Case Study of Raniganj Block, Paschim Bardhaman, West Bengal. *Model. Earth Syst. Environ.* **2018**, *4*, 1085–1110. [CrossRef]
91. De Reu, J.; Bourgeois, J.; Bats, M.; Zwertvaegher, A.; Gelorini, V.; De Smedt, P.; Chu, W.; Antrop, M.; De Maeyer, P.; Finke, P.; et al. Application of the topographic position index to heterogeneous landscapes. *Geomorphology* **2013**, *186*, 39–49. [CrossRef]
92. Jenness, J. Topographic Position Index (Tpi_jen. Avx_extension for Arcview 3. x, v. 1.3 a, Jenness Enterprises [EB/OL]. 2006. Available online: http://www.jennessent.com/arcview/tpi.htm (accessed on 7 June 2022).
93. Choubin, B.; Rahmati, O.; Soleimani, F.; Alilou, H.; Moradi, E.; Alamdari, N. Regional Groundwater Potential Analysis Using Classification and Regression Trees. In *Spatial Modeling in GIS and R for Earth and Environmental Sciences*; Elsevier: Amsterdam, The Netherlands, 2019; pp. 485–498.
94. Panahi, M.; Sadhasivam, N.; Pourghasemi, H.R.; Rezaie, F.; Lee, S. Spatial Prediction of Groundwater Potential Mapping Based on Convolutional Neural Network (CNN) and Support Vector Regression (SVR). *J. Hydrol.* **2020**, *588*, 125033. [CrossRef]
95. Rizeei, H.M.; Pradhan, B.; Saharkhiz, M.A.; Lee, S. Groundwater Aquifer Potential Modeling Using an Ensemble Multi-Adoptive Boosting Logistic Regression Technique. *J. Hydrol.* **2019**, *579*, 124172. [CrossRef]
96. Sen, Z. *Wadi Hydrology*; CRC Press: Boca Raton, FL, USA, 2008; ISBN 0429148046.
97. Chung, C.-J.F.; Fabbri, A.G. Validation of Spatial Prediction Models for Landslide Hazard Mapping. *Nat. Hazards* **2003**, *30*, 451–472. [CrossRef]
98. Saha, S. Groundwater Potential Mapping Using Analytical Hierarchical Process: A Study on Md. Bazar Block of Birbhum District, West Bengal. *Spat. Inf. Res.* **2017**, *25*, 615–626. [CrossRef]